Component-Level Polymer Composite Spot Shielding for Radiation and Thermal Management in SmallSats

Saurabh Khuje*
Dept. of Research and Development
Advanced Cooling Technologies, Inc.
Lancaster, PA, USA
saurabh.khuje@1-act.com

An Zou
Dept. of Research and Development
Advanced Cooling Technologies, Inc.
Lancaster, PA, USA
an.zou@1-act.com

Srujan Rokkam
Dept. of Research and Development
Advanced Cooling Technologies, Inc.
Lancaster, PA, USA
srujan.rokkam@1-act.com

Yue Xiao*
Department of Mechanical and Aerospace Engineering
The University of Alabama in Huntsville
Huntsville, AL, USA
yue.xiao@uah.edu

Robert Hayes
Department of Nuclear Engineering
North Carolina State University
Raleigh, NC, USA
rbhayes@ncsu.edu

Patrick Hartwell
Department of Nuclear Engineering
North Carolina State University
Raleigh, NC, USA
pjhartwe@ncsu.edu

***Abstract*—The increasing use of commercial-off-the-shelf (COTS) electronics in SmallSat platforms offers significant advantages in cost, performance, and development speed; however, radiation tolerance and thermal constraints often force conservative spacecraft-level shielding strategies. Bulk aluminum enclosures introduce substantial size, weight, and power (SWaP) penalties and frequently require entire subsystems to be over-shielded based on the most radiation-sensitive component. This paper presents a component-level radiation shielding approach for SmallSat electronics based on polymer composite spot shielding, evaluated as an alternative to full aluminum enclosures. The architecture combines a high-density metal-oxide polymer composite (MOPC) for ionizing radiation attenuation with a fiber-reinforced polymer composite (FRPC) layer engineered for in-plane thermal spreading. Together, the layers enable selective protection of radiation-sensitive components while redistributing localized heat without increasing shield thickness or electrical conductivity. Radiation attenuation measurements show that the MOPC layer achieves up to seven times higher mass attenuation efficiency than aluminum in low-energy photon regimes relevant to electron-dominated low Earth orbit environments. Environmental testing demonstrates that the composite system maintains mechanical integrity following total ionizing dose exposures up to 600 krad(Si), as well as extended thermal-vacuum cycling between -20 °C and 125 °C. Both composite layers satisfy NASA ASTM E595 outgassing requirements. System-level demonstrations using representative SmallSat electronics indicate that targeted spot shielding can reduce total radiation shielding mass by 70 - 85% compared with aluminum enclosure-based approaches, while simultaneously improving thermal behavior at the component level. These results highlight a practical pathway for reducing SWaP penalties and expanding the viable use of high-performance COTS electronics in future SmallSat missions.**

Keywords— Radiation Shielding, COTS, SmallSat, Direct Ink Writing, Thermal Management, Polymer Composites

I. Introduction

The rapid evolution of the SmallSat and CubeSat industry is largely driven by the integration of high-performance commercial-off-the-shelf (COTS) electronics. Modern system-on-chip (SoC) processors, field-programmable gate arrays (FPGAs), and high-density memory modules enable advanced onboard data processing, autonomous navigation, and high-bandwidth communications within a miniaturized form factor [1-4]. However, the transition from radiation-hardened components to COTS hardware introduces a critical vulnerability: susceptibility to ionizing radiation. Energetic particles from galactic cosmic rays and solar events can induce total ionizing dose (TID) effects and single-event phenomena that jeopardize mission reliability [1, 2, 4].

Traditionally, spacecraft designers have relied on "bulk" or "enclosure-level" shielding, typically consisting of aluminum chassis thickened to provide a safe radiation environment for the entire internal volume. This approach is increasingly incompatible with the stringent size, weight, and power (SWaP) constraints of SmallSats. Bulk shielding often leads to significant over-shielding, where the mass of the entire enclosure is dictated by the single most radiation-sensitive component on a printed circuit board (PCB) [1, 2, 4]. Furthermore, as COTS processors become more powerful, they generate localized heat loads that aluminum enclosures cannot directly mitigate, leading to thermal gradients that threaten device longevity.

To address these limitations, researchers have investigated lightweight alternatives, specifically hydrogen-rich polymers and high-Z polymer composites [5-11]. Matrices such as polyurethane or epoxy, when loaded with high atomic number (high-Z) fillers, can significantly enhance photon attenuation via the photoelectric effect while maintaining a low density compared to metallic alloys [5, 9]. While previous studies have focused on the intrinsic attenuation properties of these materials,

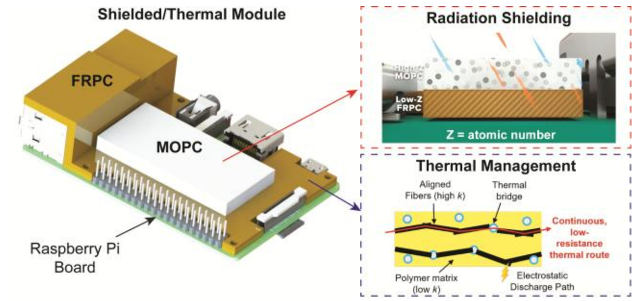

Fig. 1. Multilayer composite shielding system for SmallSat electronics. The architecture combines a high-Z Metal-Oxide Polymer Composite (MOPC) for radiation protection with a Fiber-Reinforced Polymer Composite (FRPC) for integrated thermal management and lateral heat spreading.

there is a lack of focus on how these materials can be integrated directly at the component level to solve both radiation and thermal constraints simultaneously.

This paper presents a multifunctional dual-layer polymer composite architecture designed for component-level spot shielding. By utilizing direct ink writing (DIW) additive manufacturing, we demonstrate a conformal shielding strategy that can be applied directly to sensitive electronics. This approach provides targeted radiation protection and lateral heat spreading, enabling a reduction in total shielding mass by up to 85% compared to conventional aluminum enclosures. The following sections detail the material architecture, the thermomechanical performance under space-relevant environments, and the system-level advantages for future SmallSat missions.

II. COMPOSITE ARCHITECTURE AND FABRICATION

The proposed spot-shielding system utilizes a dual-layer, multifunctional architecture designed to decouple radiation protection from the primary spacecraft structure. The system consists of a Metal-Oxide Polymer Composite (MOPC) for radiation attenuation and a Fiber-Reinforced Polymer Composite (FRPC) for thermal management (Fig. 1).

A. Multifunctional Layer Design

The MOPC layer serves as the primary radiation barrier. Gadolinium oxide (Gd_2O_3) was selected as the functional filler due to its high atomic number ($Z = 64$) and high density, which maximizes photoelectric interaction cross-sections at lower photon energies typical of electron-dominated Low Earth Orbit (LEO) environments [12]. The particles are encapsulated in a polyurethane (PU) matrix, which provides the mechanical flexibility required to withstand launch vibrations and thermal expansion.

The FRPC layer is engineered for high in-plane thermal conductivity (k_{in}). It utilizes a hybrid filler approach: carbon fibers provide the primary conduction pathways, while copper particles act as "thermal bridges" to reduce interfacial resistance between adjacent fibers. This layer is designed to sit between the electronic component and the MOPC shield, acting as a lateral heat spreader that moves thermal energy away from the junction toward the PCB ground planes.

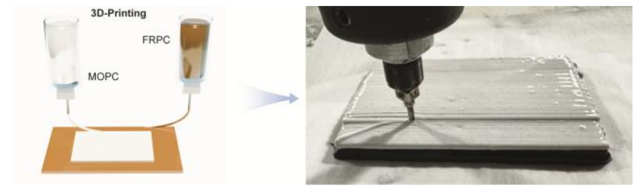

Fig. 2. DIW additive manufacturing process. The image illustrates the transition from the dual-ink design (left) to the automated conformal deposition of the composite shield (right), enabling targeted protection of sensitive silicon junctions.

B. Direct Ink Writing (DIW) Integration

Unlike traditional metallic shields that require complex machining, these composites are deposited via DIW, a syringe-based extrusion process. This additive manufacturing approach offers three critical advantages for SmallSat integration:

- Conformality: The shielding material can be printed directly onto the irregular geometries of COTS components (e.g., SoC packages, inductors, or capacitors).
- Selectivity: Shielding thickness can be varied across a single board, applying 3.0 mm of protection to a sensitive FPGA while using only 1.0 mm for more robust components.
- Low SWaP-C: The process eliminates the need for heavy mechanical fasteners, as the polyurethane matrix provides inherent adhesion to the PCB substrate.

For this study, MOPC formulations were loaded at 72 wt.% Gd_2O_3 and FRPC formulations at 43 wt.% carbon fiber to optimize the balance between functional performance and extrudability (Fig. 2). Multi-layer structures were fabricated using a 1.5 mm nozzle at printing speeds of 35 - 40 mm s^{-1}, enabling rapid prototyping of shielding geometries tailored to specific SmallSat avionics modules [13].

III. RADIATION AND THERMAL PERFORMANCE

A. Radiation Attenuation Efficiency

The radiation performance of the MOPC layer is intrinsically linked to the uniformity of its microstructure. As shown in Fig. 3, the optimized DIW process produces a dense, void-free composite (72 wt.% Gd_2O_3) which is essential for preventing radiation leakage and ensuring predictable attenuation. Experimental measurements of the mass attenuation coefficient (μ_m) show that this high-Z loading enables

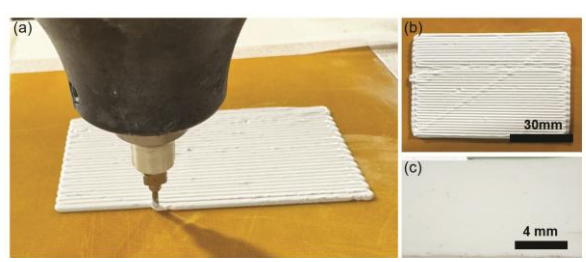

Fig. 3. DIW-printed MOPC radiation shielding samples. (a) Syringe-extrusion process, (b) top-down view of the printed geometry, and (c) cross-sectional analysis. The high packing density of the Gd_2O_3 fillers within the matrix ensures uniform photon attenuation across the shielded area.

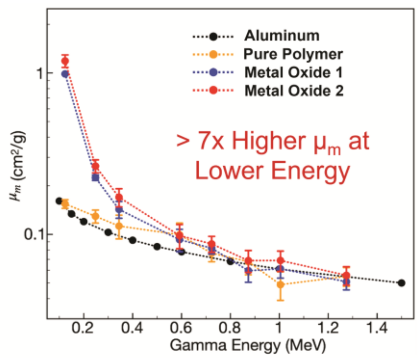

Fig. 4. Comparison of mass attenuation coefficients (μ_m) derived from MCNP6 simulations for Aluminum, pure polymer, and two MOPC formulations. The MOPC layers demonstrate a > 7× increase in attenuation efficiency compared to Aluminum in the low-energy gamma regime (< 200 keV). This performance gap highlights the effectiveness of high-Z loading for mitigating the electron-dominated radiation environments typical of LEO.

exceptional performance in the low-energy regime (below 100 keV), relevant to secondary bremsstrahlung in electron-rich LEO environments.

In this regime, the MOPC achieves over seven times higher mass attenuation than conventional aluminum [12, 14]. This is primarily due to the high atomic number of Gadolinium ($Z = 64$) which significantly increases the probability of photoelectric absorption. These material properties were integrated into MCNP6 transport simulations (Fig. 4) to translate intrinsic attenuation into mission-level dose reductions. The results indicate that replacing bulk aluminum with targeted MOPC spot shielding provides equivalent protection to sensitive silicon junctions while drastically reducing the total shielding mass [13].

B. Integrated Thermal Management

A common failure point for shielded COTS electronics is the "thermal blanket" effect, where thick shielding traps heat generated by high-speed processors. The FRPC layer addresses this by providing an engineered thermal pathway (Fig. 5a-d). During the DIW process, shear forces within the extrusion nozzle induce directional alignment of the carbon fibers along the printing path [13]. This creates an anisotropic thermal response:

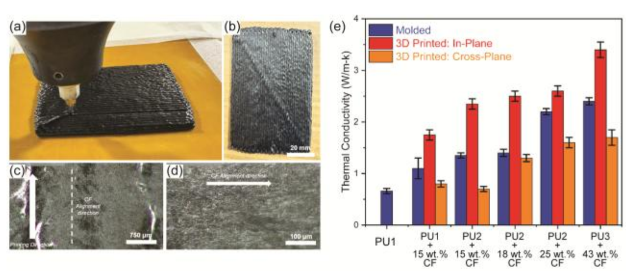

Fig. 5. Thermal performance and anisotropic properties of the FRPC layer. (a) DIW deposition of the carbon-fiber-reinforced composite. (b) Macro view of the printed thermal test coupon. (c-d) Optical micrographs showing high degrees of fiber alignment along the print path induced by nozzle shear forces. (e) Comparison of thermal conductivity for molded vs. 3D-printed samples. The 3D-printed "*in-plane*" configuration achieves a maximum conductivity of 3.4 W/m-K, significantly outperforming isotropic molded counterparts due to engineered fiber orientation.

- In-plane conductivity: Measured at 3.0 - 3.8 W m^{-1} K^{-1}, which is an order of magnitude higher than unfilled polymers (Fig. 5e).
- Thermal Bridging: The inclusion of copper particles as bridging fillers reduces interfacial resistance, enabling heat to spread laterally across the shield surface rather than accumulating at the component-shield interface.

This dual-functionality ensures that as the MOPC layer attenuates radiation, the underlying FRPC layer actively redistributes localized hotspots, maintaining the device junction temperature within reliable operating limits without requiring additional active cooling or increased shield volume.

IV. ENVIRONMENTAL DURABILITY AND QUALIFICATION

To ensure compatibility with the rigors of spaceflight, the dual-layer composite system underwent extensive environmental testing focusing on ionizing radiation stability, thermal-vacuum (TVAC) endurance, and vacuum outgassing.

A. Radiation Stability and TID Exposure

Polymer-based shields must maintain structural integrity under prolonged exposure to ionizing radiation. Composite specimens were subjected to Total Ionizing Dose (TID) testing up to 600 krad(Si) to simulate multi-year LEO missions (Fig. 6). Post-exposure mechanical testing showed no evidence of embrittlement, cracking, or interfacial degradation [13, 15]. The high loading of Gd_2O_3 particles contributes to this stability by absorbing a significant fraction of the incident energy, thereby protecting the polyurethane matrix from chain scission and radical formation. Tensile strength measurements remained consistent across the dose range, confirming that the shield remains mechanically robust throughout its operational life.

B. Thermal-Vacuum (TVAC) Cycling

SmallSats experience rapid thermal cycling as they transition between sunlight and eclipse. To evaluate thermomechanical fatigue, shielded assemblies (including a Raspberry Pi representative module) were subjected to 500 thermal cycles between -20 °C and 125 °C under a high vacuum (10^{-5} torr).

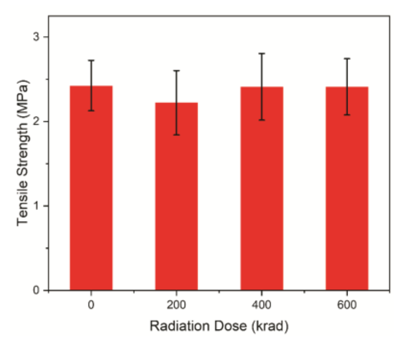

Fig. 6. Tensile strength of the MOPC shielding as a function of total ionizing dose (TID). The material maintains a stable mechanical profile up to 600 krad(Si), with no statistically significant degradation in strength ($N = 6$ per exposure). This stability confirms that the high-Z filler loading effectively protects the polymer matrix from radiation-induced embrittlement, ensuring long-term structural integrity in LEO and deep-space environments.

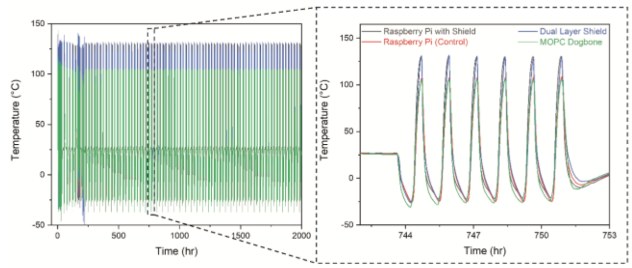

Fig. 7. Thermal-vacuum (TVAC) endurance testing of the composite shielding system. (Left) Continuous temperature profile over 2,000 hours of operation, encompassing 500 cycles between -20 °C and 125 °C. (Right) Magnified view of representative cycles showing stable thermal response across the Raspberry Pi assembly, the dual-layer shield, and MOPC test coupons. The consistent overlap in thermal profiles confirms that the integrated shield maintains mechanical and thermal contact without delamination or performance degradation throughout extended cycling.

Despite the mismatch in coefficients of thermal expansion (CTE) between the fillers and the polymer, the polyurethane matrix provided sufficient elasticity to dissipate internal stresses. No delamination or loss of adhesion to the PCB substrate was observed. The stable thermal profiles recorded across 500 cycles confirm that the interfacial bond between the MOPC and FRPC layers remains intact, ensuring consistent thermal and radiation protection over the mission duration (Fig. 7).

C. *Outgassing and Contamination Control*

Strict adherence to NASA outgassing standards is mandatory to prevent the deposition of volatile condensable materials on sensitive payloads like cameras or solar cells. Both the MOPC and FRPC layers were tested in accordance with ASTM E595.

- Total Mass Loss (TML): Measured at 0.66% for MOPC and 0.51% for FRPC (well below the 1.0% limit).
- Collected Volatile Condensable Material (CVCM): Estimated at ≤ 0.06%, comfortably below the 0.1% threshold [15].

These results verify that the material system is "space-grade" and safe for integration into multi-instrument SmallSat platforms without the risk of molecular contamination.

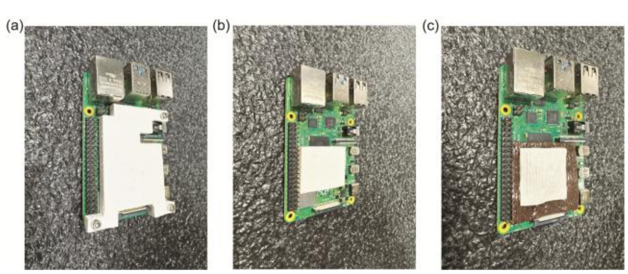

Fig. 8. Representative deployment strategies for component-level shielding on SmallSat electronics. (a) Full-Surface Encapsulation for maximum environmental and radiation protection across the entire PCB. (b) Localized Spot Shielding targeting specific radiation-sensitive COTS components to minimize mass. (c) Bilayer Multifunctional Shielding integrating the MOPC radiation layer with an underlying FRPC thermal spreader for high-power, sensitive processors.

V. SYSTEM-LEVEL INTEGRATION AND MASS OPTIMIZATION

The primary value proposition of the dual-layer composite architecture is the transition from "box-level" to "component-level" shielding. This shift allows SmallSat designers to optimize the spacecraft mass budget by targeting only the most vulnerable silicon junctions.

A. *Deployment Strategies*

To evaluate the practical benefits of the proposed system, three shielding configurations were integrated onto a representative high-performance COTS electronics platform:

1. Full-Surface Encapsulation: Coating the entire PCB for maximum protection and environmental sealing (Fig. 8a).
2. Localized Spot Shielding: Applying MOPC only to the primary processor and memory modules (Fig. 8b).
3. Bilayer Spot Shielding: Integrating the MOPC radiation layer with the FRPC thermal spreader for high-power components (Fig. 8c).

DIW enabled these structures to conform to the irregular heights and geometries of the surface-mount components while maintaining clear access to critical connectors and ports, a significant advantage over rigid metallic covers.

B. *Mass Comparison and SWaP Benefits*

The mass of each composite configuration was compared against a traditional 6061-T6 aluminum enclosure designed to provide an equivalent radiation dose reduction. The results highlight a dramatic reduction in the mass budget (Fig. 9):

- Traditional Aluminum Enclosure: ~153 g
- MOPC Spot Shielding: ~22 g (85% reduction)
- Bilayer MOPC-FRPC Shielding: ~45 g (70% reduction)

By reducing the shielding mass from 153 g to 22 g, a 3U CubeSat designer could reallocate over 130 g of the mass budget to additional battery cells, larger reaction wheels, or more sensitive scientific instrumentation. Furthermore, the bilayer approach provides integrated thermal management that a passive aluminum box cannot match, enabling the use of higher-clock-speed COTS processors in thermally constrained SmallSat buses.

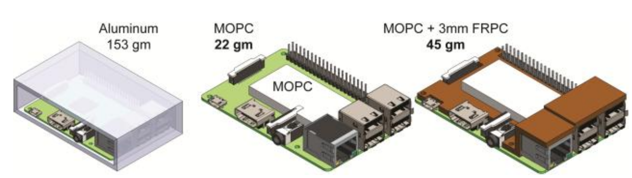

Fig. 9. System-level mass comparison between traditional aluminum shielding and the proposed polymer composite spot-shielding architecture. Replacing a 153 g bulk aluminum enclosure with a targeted 22 g MOPC spot shield achieves an 85% reduction in shielding mass. Even with the addition of a 3 mm FRPC thermal management layer (45 g), the system provides a 70% mass saving while offering integrated thermal control that the passive aluminum box lacks.

VI. CONCLUSION

The transition toward high-performance, COTS-intensive SmallSat architecture requires a fundamental shift in how we approach radiation and thermal protection. This work has demonstrated that a multifunctional, additively manufactured polymer composite system can effectively replace traditional, mass-heavy aluminum shielding while simultaneously addressing the localized thermal constraints of modern electronics. The MOPC-FRPC architecture offers three transformative advantages for the SmallSat industry:

1. Mass Efficiency: By moving to a component-level "spot shielding" strategy, mission designers can achieve up to an 85% reduction in shielding mass compared to conventional enclosures.
2. Integrated Functionality: The system does not merely block radiation; the engineered FRPC layer acts as a high-conductivity thermal spreader (up to 3.8 W m^{-1} K^{-1}), preventing the thermal "blanketing" effects that often plague traditional shielding methods.
3. Flight Readiness: With successful validation through 500 TVAC cycles, 600 krad(Si) TID exposure, and compliance with NASA ASTM E595 outgassing standards, the material system is flight-ready and compatible with the most sensitive spacecraft environments.

By utilizing DIW, this approach provides a scalable and conformal manufacturing pathway that can be tailored to any PCB layout. As SmallSat missions push further into high-radiation orbits and deep-space environments, the ability to selectively protect and cool advanced processors will be a critical enabler. This multifunctional composite architecture provides a practical, low-SWaP solution for ensuring the reliability of the next generation of space-based computational power.

ACKNOWLEDGMENT

This research was funded by the U.S. Department of Energy (DOE) SBIR Program via Phase I and Phase II Awards DE-SC0022897. Additionally, the authors thank Prof. Robert B. Hayes and his research group at North Carolina State University for their technical expertise and contributions to the radiation modeling and shielding analysis.

REFERENCES

[1] J. Miller, C. Zeitlin, F. Cucinotta, L. Heilbronn, D. Stephens, and J. Wilson, "Benchmark studies of the effectiveness of structural and internal materials as radiation shielding for the international space station," *Radiation research,* vol. 159, no. 3, pp. 381-390, 2003.

[2] M. R. Shavers *et al.*, "Implementation of ALARA radiation protection on the ISS through polyethylene shielding augmentation of the Service Module Crew Quarters," *Advances in Space Research,* vol. 34, no. 6, pp. 1333-1337, 2004.

[3] F. A. Cucinotta, M.-H. Y. Kim, and L. J. Chappell, "Evaluating shielding approaches to reduce space radiation cancer risks," *NASA Technical Memorandum,* vol. 217361, 2012.

[4] T. C. Slaba, A. A. Bahadori, B. D. Reddell, R. C. Singleterry, M. S. Clowdsley, and S. R. Blattnig, "Optimal shielding thickness for galactic cosmic ray environments," *Life Sciences in space research,* vol. 12, pp. 1-15, 2017.

[5] S. Nambiar and J. T. Yeow, "Polymer-composite materials for radiation protection," *ACS applied materials & interfaces,* vol. 4, no. 11, pp. 5717-5726, 2012.

[6] M. Ambika, N. Nagaiah, and S. Suman, "Role of bismuth oxide as a reinforcer on gamma shielding ability of unsaturated polyester based polymer composites," *Journal of Applied Polymer Science,* vol. 134, no. 13, 2017.

[7] R. R. Bhosale, C. V. More, D. K. Gaikwad, P. P. Pawar, and M. N. Rode, "Radiation shielding and gamma ray attenuation properties of some polymers," *Nuclear Technology and Radiation Protection,* vol. 32, no. 3, pp. 288-293, 2017.

[8] A. Wozniak, V. Ivanov, O. Zhdanovich, V. Nazarov, and A. Yegorov, "Modern approaches to polymer materials protecting from ionizing radiation," *Orient. J. Chem,* vol. 33, 2018.

[9] E. B. Podgoršak, "Energy transfer and energy absorption in photon interaction with matter," in *Compendium to Radiation Physics for Medical Physicists: 300 Problems and Solutions*: Springer, 2014, pp. 515-580.

[10] N. N. Azman, S. Siddiqui, R. Hart, and I. Low, "Effect of particle size, filler loadings and x-ray tube voltage on the transmitted x-ray transmission in tungsten oxide—epoxy composites," *Applied radiation and isotopes,* vol. 71, no. 1, pp. 62-67, 2013.

[11] E. Eren Belgin and G. Aycik, "Preparation and radiation attenuation performances of metal oxide filled polyethylene based composites for ionizing electromagnetic radiation shielding applications," *Journal of Radioanalytical and Nuclear Chemistry,* vol. 306, no. 1, pp. 107-117, 2015.

[12] Q. Chang, S. Guo, and X. Zhang, "Radiation shielding polymer composites: Ray-interaction mechanism, structural design, manufacture and biomedical applications," *Materials & Design,* vol. 233, p. 112253, 2023.

[13] Y. Xiao, A. Zou, D. Carlson, A. Rahman, and P. Zhang, "3D-Printed Polymer-Based Conformal Space Radiation Shield with Heat Dissipation," 2024.

[14] K. Shahzad *et al.*, "Views on radiation shielding efficiency of polymeric composites/nanocomposites and multi-layered materials: current state and advancements," *Radiation,* vol. 3, no. 1, pp. 1-20, 2022.

[15] M. P. Easton, A. C. Labatete-Goeppinger, J. D. Fowler, and D.-L. Liu, "Identification of collected volatile condensable material (CVCM) from ASTM E595 of silicone damper fluid," in *Systems Contamination: Prediction, Measurement, and Control 2014*, 2014, vol. 9196: SPIE, pp. 61-70.